A Long-Lived M-Like State of Phoborhodopsin that Mimics the Active State

Yuki Sudo,*† Tatsuya Nishihori,† Masayuki Iwamoto,†‡ Kazumi Shimono,†§ Chojiro Kojima,¶ and Naoki Kamo†
*Division of Biological Science, Graduate School of Science, Nagoya University, Chikusa-ku, Nagoya 464-8602, Japan; †Laboratory of Biophysical Chemistry, Graduate School of Pharmaceutical Sciences, Hokkaido University, Sapporo 060-0812, Japan; ‡Division of Molecular Physiology and Biophysics, Department of Morphological and Functional Biomedical Science, Faculty of Medical Science, University of Fukui, Matsuoka 910-1193, Japan; §RIKEN Genomic Sciences Center, 1-7-22 Suehiro-cho, Tsurumi, Yokohama 230-0045, Japan; and ¶Nara Institute of Science and Technology, 8916-5 Takayama, Ikoma, Nara 630-0192, Japan

ABSTRACT *Pharaonis* phoborhodopsin (ppR, also called *pharaonis* sensory rhodopsin II) is a seven transmembrane helical retinal protein. ppR forms a signaling complex with *pharaonis* Halobacterial transducer II (pHtrII) in the membrane that transmits a light signal to the sensory system in the cytoplasm. The M-state during the photocycle of ppR ($\lambda_{max} = 386$ nm) is one of the active (signaling) intermediates. However, progress in characterizing the M-state at physiological temperature has been slow because its lifetime is very short (decay half-time is ~1 s). In this study, we identify a highly stable photoproduct that can be trapped at room temperature in buffer solution containing *n*-octyl-β-D-glucoside, with a decay half-time and an absorption maximum of ~2 h and 386 nm, respectively. HPLC analysis revealed that this stable photoproduct contains 13-*cis*-retinal as a chromophore. Previously, we reported that water-soluble hydroxylamine reacts selectively with the M-state, and we found that this stable photoproduct also reacts selectively with that reagent. These results suggest that the physical properties of the stable photoproduct (named the M-like state) are very similar with the M-state during the photocycle. By utilizing the high stability of the M-like state, we analyzed interactions of the M-like state and directly estimated the pK_a value of the Schiff base in the M-like state. These results suggest that the dissociation constant of the $ppR_{M\text{-}like}$/pHtrII complex greatly increases (to 5 μM) as the pK_a value greatly decreases (from 12 to 1.5). The proton transfer reaction of ppR from the cytoplasmic to the extracellular side is proposed to be caused by this change in pK_a.

INTRODUCTION

Pharaonis phoborhodopsin (ppR) from *Natronomonas (Natronobacterium) pharaonis* is a seven-transmembrane helical protein that uses all-*trans*-retinal as a chromophore, whereby it binds through a PSB (protonated Schiff base) (1). Asp-75 of ppR serves as a counterion of the PSB. ppR forms a signaling complex with the pHtrII, and transmits light signals to pHtrII through the change in such interaction (2). pHtrII is a two-transmembrane helical protein that belongs to the family of two-transmembrane helical methyl-accepting chemotaxis proteins in *Escherichia coli* (3). It is well known that methyl-accepting chemotaxis proteins exist as homodimers composed of ~50–60 kDa subunits and form ternary complexes with CheA and CheW. pHtrII eventually activates the phosphorylation cascades that modulate flagellar motors (4). Using those signaling systems, the bacteria avoid harmful near-UV light ($\lambda < 520$ nm).

ppR and pHtrII are stable in membranes and in various detergent micelles (5,6), and expression systems using *E. coli* can provide large amounts of those proteins (7). Therefore, ppR and pHtrII have been well characterized recently as a model for membrane proteins (for reviews, see Sudo et al. (2) and Klare et al. (8)). The dark-state crystal structures of ppR alone, the ppR/pHtrII complex, and the high-resolution structure of the K and M states of the ppR/pHtrII complex have been reported (9–12). Our group and others have demonstrated a 1:1 stoichiometry and binding parameters in the ppR/pHtrII complex under various conditions (6,8,13,14). Of particular importance for the interaction between ppR and pHtrII are the hydrogen-bonding networks between Tyr-199^{ppR} and Asn-74, between Thr-189 and Glu-43/Ser-62, and the phenolic ring of Tyr-199 and Phe-28^{pHtrII} (6,15,16). Furthermore, the importance of Asp-193^{ppR}, Thr-204^{ppR}, and the linker region of pHtrII for the interaction has also been investigated (17–19).

ppR maximally absorbs light at 498 nm (20), which triggers the *trans-cis* isomerization of the retinal chromophore. Relaxation of the retinal leads to functional processes during the photocycle. Thus, the active intermediates of the ppR/pHtrII complex are the M- and O-intermediates (21). However, characterization of the M intermediate is less advanced because its lifetime is very short (decay half-time ~1 s). Therefore, to allow detailed study of the activation process, it is necessary to trap the stable active state at physiological temperature. By characterizing the highly stable state, new information about the activation process of proteins could be investigated.

In this study, we report that when ppR is activated by constitutive light stimuli in a buffer solution containing *n*-octyl-β-D-glucoside (OG) as a detergent, a highly stable photoproduct (termed the M-like state) can be trapped at room

Submitted November 6, 2007, and accepted for publication February 8, 2008.

Address reprint requests to Yuki Sudo, Division of Biological Science Graduate School of Science Nagoya University Chikusa-ku, Nagoya 464-8602, Japan. Tel.: 81-52-789-2993; Fax: 81-52-789-3001; E-mail: 4sudo@bunshi4.bio.nagoya-u.ac.jp.

Editor: Janos K. Lanyi.

0006-3495/08/07/753/08 $2.00

doi: 10.1529/biophysj.107.125294

temperature (25°C). The half-time of the decay is ~2 h, and the absorption maximum is 386 nm. HPLC analysis reveals that this stable photoproduct uses 13-*cis*-retinal as a chromophore. Previously, we have reported that water-soluble hydroxylamine reacts selectively with the M-state (22,23), and we show that the stable photoproduct also reacts selectively with that reagent. These results suggest that the physical properties of the stable photoproduct (the M-like state) are very similar to those of the M-state during the photocycle. By utilizing the higher stability of the M-like state, we analyzed the interaction between ppRM and pHtrII and estimated the pK_a value of the Schiff base in the M-mimicked state.

MATERIALS AND METHODS

Sample preparation

Expression plasmids of ppR and pHtrII were constructed as previously described (6,15). Truncated pHtrII expressed from positions 1 to 159 was used instead of the whole protein because this truncated form is enough to permit interaction with ppR (6,11,16,24). Hereafter, pHtrII signifies the truncated protein.

ppR and pHtrII were expressed in *E. coli* BL21 (DE3) cells. The preparation of crude membranes and the purification of proteins were performed as previously described (6,15). The samples were concentrated using an Amicon Ultra (Millipore, Bedford, MA) and were exchanged completely by dialysis against a buffer solution (50 mM KCl, 10 mM Citrate (pH 5.0), and 1% OG) for 1 week using a 10-kDa cutoff dialysis cassette (Daiichi Pure Chemicals, Tokyo, Japan). We monitored the concentration of detergents using NMR (19). Protein concentrations of ppR and pHtrII were determined using the molar extinction coefficients of 498 nm (40,000 M^{-1} cm^{-1}) and 280 nm (Tyr 1420 M^{-1} cm^{-1}), respectively. Because the molecular coefficient of pHtrII at 280 nm is small (4320 M^{-1} cm^{-1}), the pHtrII concentration determined was confirmed by the result of band intensity in the SDS-PAGE gel. The ppR was used as a standard. For preparation of the ppR/pHtrII complex, the purified ppR and pHtrII proteins were mixed in various molar ratios (see below) followed by incubation for 1 h at 4°C.

Absorption spectroscopy and HPLC analysis

For measurement of the M-like state formation, spectra were obtained using a V-560 spectrophotometer (Japan Spectroscopic, Tokyo, Japan) under constant illumination with a Y52 filter (Toshiba, Tokyo, Japan) (>500 nm). The reaction mixture was irradiated with an intensity of 5 W/m^2. After the illumination, data of the reverse reaction from the M-like to the ground state were collected in the dark with the same spectrophotometer. Samples were suspended in a buffer solution containing 50 mM KCl, 10 mM citrate (pH 5.0), and 1% OG. The retinal isomer ratio of ppR pigments was determined using HPLC (model 800 series, Japan Spectroscopic). Extraction of the retinal oxime from the sample was carried out using hexane after denaturation by methanol and 500 mM hydroxylamine. HPLC was performed using the same procedures and methods as described previously (25).

Reaction with hydroxylamine

Sample proteins were suspended in the buffer solution described above and were immediately supplemented with 50 mM hydroxylamine after constant background illumination (>520 nm) for the M-like state and in the dark for the ground state. The formation of the retinal oxime, reaction of ppR with hydroxylamine, was monitored by spectrophotometer. Experiments were done at 25°C.

Estimation of pK_a of the Schiff base in the M-like state

After the constant illumination in the presence of 1% OG at pH 5.0 (10 mM citrate), the pH was adjusted to 1.2 using concentrated H_2SO_4 and a mixture of six buffers (containing citric acid, MES, HEPES, MOPS, CHES, and CAPS at 10 mM each) because that buffer composition has the same buffer capacity for the wide range of pH values (2–9) used in this study. Titration of the PSB started from pH 1.2 to 3.9 and was adjusted by the addition of concentrated NaOH, and the absorption spectra were then measured. Each series of titrations took 15 min, and the transition from the M-like state to the ground state was ignored because the half-time of the M-like state is ~2 h.

RESULTS

Formation of a highly stable photoproduct

When ppR was illuminated by constant light in a buffer solution containing OG as a detergent, a photoproduct with a λ_{max} of 386 nm was trapped at room temperature (25°C) (Fig. 1). The spectra were somewhat noisy because these measurements were done under the light illumination. With an increase in the time of light illumination, the absorption band at 386 nm increased as a result of the formation of photoproduct. Fig. 1 *b* shows difference spectra. These two spectra are proportional with an isosbestic point of 410 nm, which implies that a photo-dependent transition from the ground state ($\lambda_{max} = 500$) to photoproduct ($\lambda_{max} = 386$ nm) occurs. For bR, this photoproduct was not trapped or detected in this buffer condition (data not shown). However, Imasheva et al. (26) reported that a somewhat similar photoproduct formed at high pH resulted in the accumulation of a long-lived photoproduct absorbing at 362 nm for proteorhodopsin.

After 120 min of illumination, the absorption spectra were measured. Fig. 2 shows the reverse reaction from a photoproduct to the ground state of ppR. With an increase in time, the absorption band at 500 nm caused by the reformation of ground state ppR increased. After 1200 min, all photoproducts had reverted to the ground state. Fig. 2 *b* shows difference spectra of this reaction. These two spectra are proportional with an isosbestic point of 410 nm, which suggests that the ground state ppR turns to a highly stable photoproduct on constant photoillumination, after which this photoproduct returns to the ground state ppR. The molar extinction coefficient at 386 nm was determined as 12,000 M^{-1} cm^{-1} using relative absorbance with the ground state (40,000 M^{-1} cm^{-1}) (27) (see Figs. 1 *b* and 2 *b*).

We analyzed the time courses of these transitions from the ground state to a photoproduct (spectral change from 500 to 386 nm) and from the photoproduct back to the ground state (spectral change from 386 to 500 nm). The rate constants of the formation of photoproduct were 0.013 ± 0.002 min^{-1} (at 500 nm) and 0.011 ± 0.002 min^{-1} (at 386 nm), whereas those of the return to the ground state were 0.005 ± 0.001 min^{-1} (at 500 nm) and 0.006 ± 0.001 min^{-1} (at 386 nm). These data could be fit with a single exponential equation.

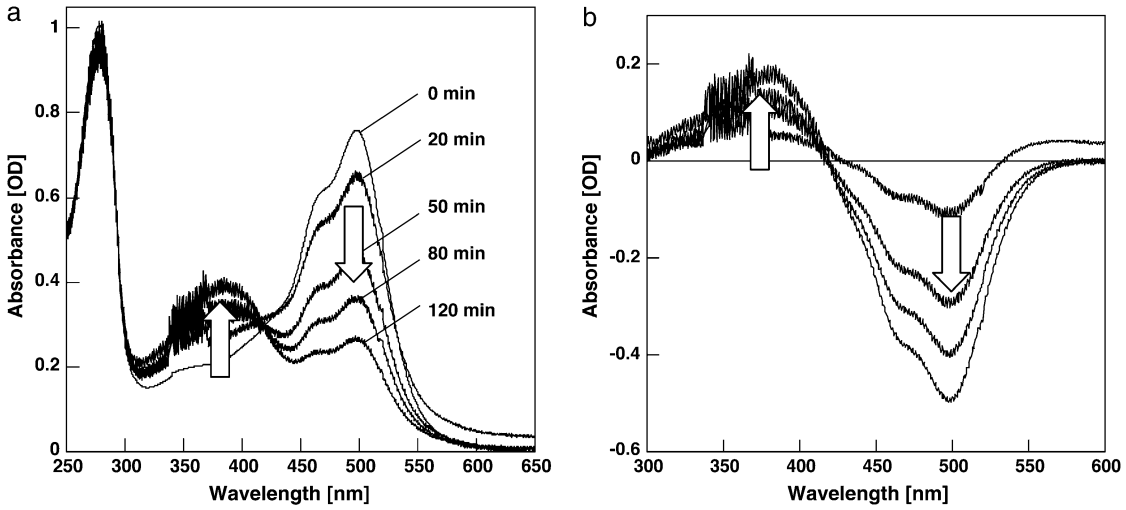

FIGURE 1 Light-induced spectral changes of ppR. (*a*) Time-dependent spectral changes of ppR. The spectra were recorded at 0, 20, 50, 80, and 120 min. Spectra except for 0 min were noisy because we monitored these spectra under constant light illumination. (*b*) Difference absorption spectra. The reaction mixture was irradiated with an intensity of 5 W/m^2. ppR at 18 μM was suspended in buffer at pH 5.0 (see Materials and Methods) at 25°C.

Biophysical properties of a highly stable photoproduct, the M-like state

What is the highly stable photoproduct? The absorbance maximum of this metastable state is almost the same as that of the M state during the photocycle. In the dark, ppR has all-*trans*-retinal (25), whereas ppR in the M state during the photocycle has 13-*cis*-retinal as a chromophore (28). Fig. 3 shows the correlation between retinal configuration and increase or decrease of absorption at 500 (*open circles*) and 386 nm (*solid circles*), respectively. With an increase in the absorption at 386 nm, the amount of 13-*cis*-retinal increased. Both values were well correlated, which strongly suggests that the metastable photoproduct has 13-*cis*-retinal as a chromophore. Hereafter, this photoproduct having 13-*cis* retinal is called the M-like state.

Previously, we reported that water-soluble hydroxylamine attacked the Schiff base selectively at the M state of ppR to bleach the pigment (22,23). The increase in this reactivity was mainly caused by an increase in the accessibility of this reagent to the hydrophobic moiety of the protein. Therefore, the reactivity of hydroxylamine is a good indicator for the conformational change of the protein (ppR). Fig. 4 shows the reactivity of hydroxylamine with $ppR_{M\text{-like}}$. A decrease in absorbance at 400 nm and a concomitant increase in absorbance at 345 nm were observed. The reactivity with the M-like state was much higher than that of the ground state (Fig. 4). This property was similar to the M state during the photocycle, indicating that the conformational change in the protein in the M-like state is similar to that of the M state.

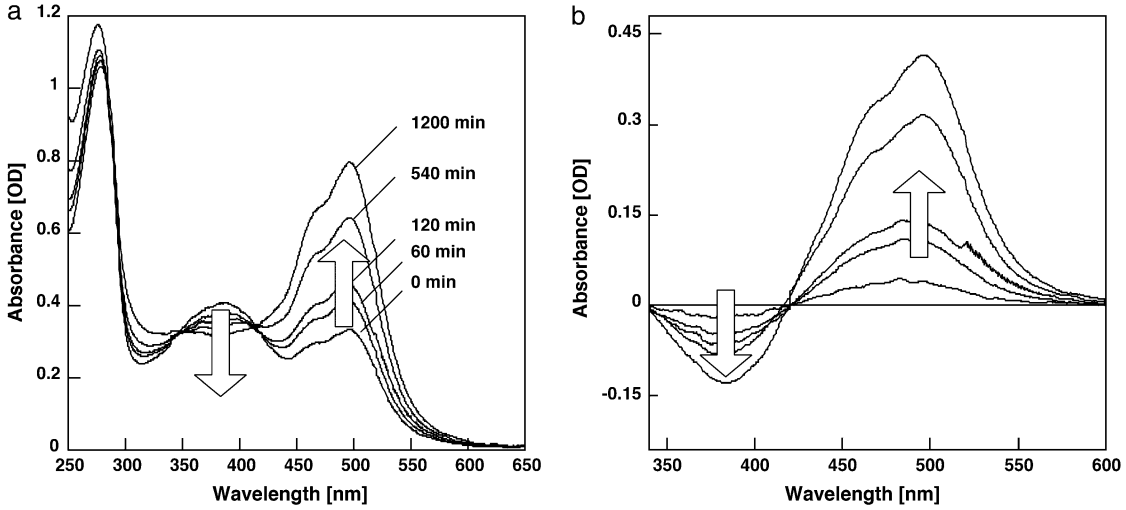

FIGURE 2 Spectral transition from a photoproduct (λ_{max} = 386 nm) to the ground state (λ_{max} = 500 nm) of ppR. (*a*) Time-dependent spectral changes of ppR. The spectra were recorded at 0, 60, 120, 540, and 1200 min. (*b*) Difference absorption spectra. Experimental conditions were as described for Fig. 1.

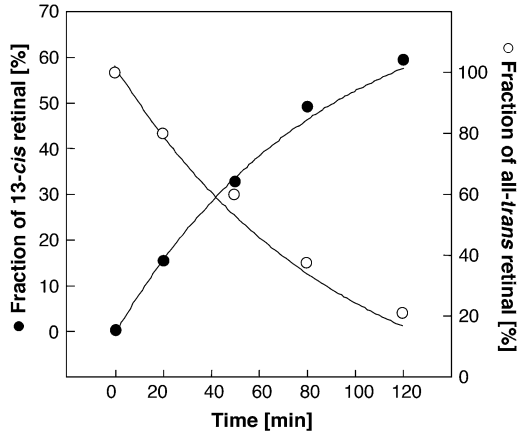

FIGURE 3 Chromophore configuration of the photoproduct (the M-like state). The detection beam was set at 360 nm. Samples were collected and extracted from the protein at 0, 20, 60, 80, and 120 min. The fraction of 13-*cis*- and all-*trans*-retinal was determined by calculation of molar compositions from the areas of the peaks in the HPLC patterns. Solid lines that indicate light-induced absorbance changes were reproduced from Fig. 3 *a*. The fraction of 13-*cis*- and all-*trans*-retinal were well correlated with absorbance changes of the decrease of the ground state and the increase of the photoproduct (the M-like state).

Interaction between pHtrII and the mimicking M (active) state

The ppR samples (8 μM) with or without pHtrII (40 μM) were irradiated by yellow light through a Y52 filter for 360 min. The back reaction from the M-like state to the ground state in the presence or absence of purified pHtrII was monitored as an increase in absorbance at 500 nm (Fig. 5 *a*). The transition curves could be fit with a single exponential equation (Fig. 5, *solid lines*). The transition at 5-, 10-, 20-, and 30-fold molar excess of pHtrII always followed a single exponential transition with the same rate constant, which implies that all ppR proteins form complexes with pHtrII. The transition rate constant of ppR alone was 0.006 $\pm$ 0.001 min^{-1}, whereas that of the complex was 0.017 $\pm$ 0.002 min^{-1}, almost threefold faster than that of ppR alone.

By utilizing the high stability of the M-like state, we were able to analyze the interaction between $\text{ppR}_{\text{M-like}}$ and pHtrII. To estimate the K_D value, we prepared samples having varying concentrations of ppR proteins (5, 10, 15, 20, 25, 30, 35, 40 μM) and pHtrII (25 μM). The kinetic traces of the transition from the M-like to the ground state, obtained by monitoring at 500 nm, were analyzed with Eq. 1, describing the transition by a sum of two components. This is obvious because this sample may contain free ppR, ppR/pHtrII, and free pHtrII, the former two being active in the UV-Vis spectrum with different transition kinetics.

$$\Delta\text{Absorbance} = (a + b) - (c \times \exp^{-k1t} + d \times \exp^{-k2t}). \quad (1)$$

The kinetic constants k_1 (reaction rate of $\text{ppR}_{\text{M-like}}$) and k_2 (reaction rate of the $\text{ppR}_{\text{M-like}}$/pHtrII complex) were almost constant for all experimental data, and furthermore, they were equal to those of $\text{ppR}_{\text{M-like}}$ alone and of the $\text{ppR}_{\text{M-like}}$/pHtrII complex. The amplitudes in Eq. 1, c and d, are considered to be proportional to the concentrations of the free $\text{ppR}_{\text{M-like}}$ and the $\text{ppR}_{\text{M-like}}$/pHtrII complex. The binding parameters were analyzed according to the scheme shown in Eq. 2 (see below), and the fitting was performed using Origin software (Microcal Software, Northampton, MA) to evaluate the binding parameters.

The binding parameters were estimated using the same binding scheme as follows:

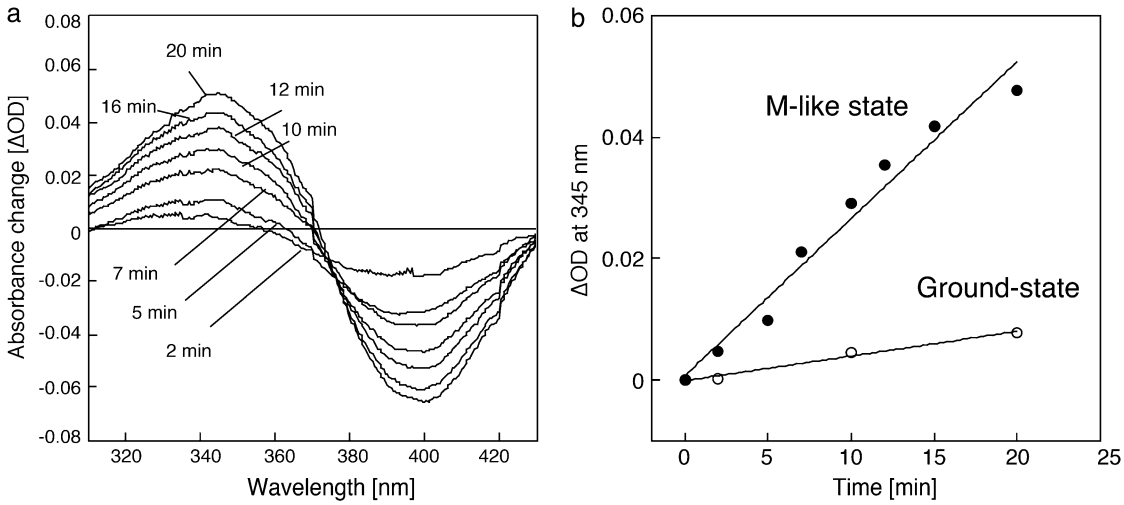

FIGURE 4 (*a*) Photoinduced difference spectra of $\text{ppR}_{\text{M-like}}$. (*b*) Reactivity of the ground states of ppR (*open circles*) and $\text{ppR}_{\text{M-like}}$ (*solid circles*) with hydroxylamine. For $\text{ppR}_{\text{M-like}}$, 50 mM hydroxylamine was added in buffer solution after constant illumination of ppR for 120 min. For the ground state of ppR, 50 mM hydroxylamine was also added in buffer solution. For measurement of the reaction of ppR with hydroxylamine, time-dependent absorbance changes at 345 nm were monitored. The slopes are: 0.0026 min^{-1} for the M-like state and 0.0004 min^{-1} for the ground state.

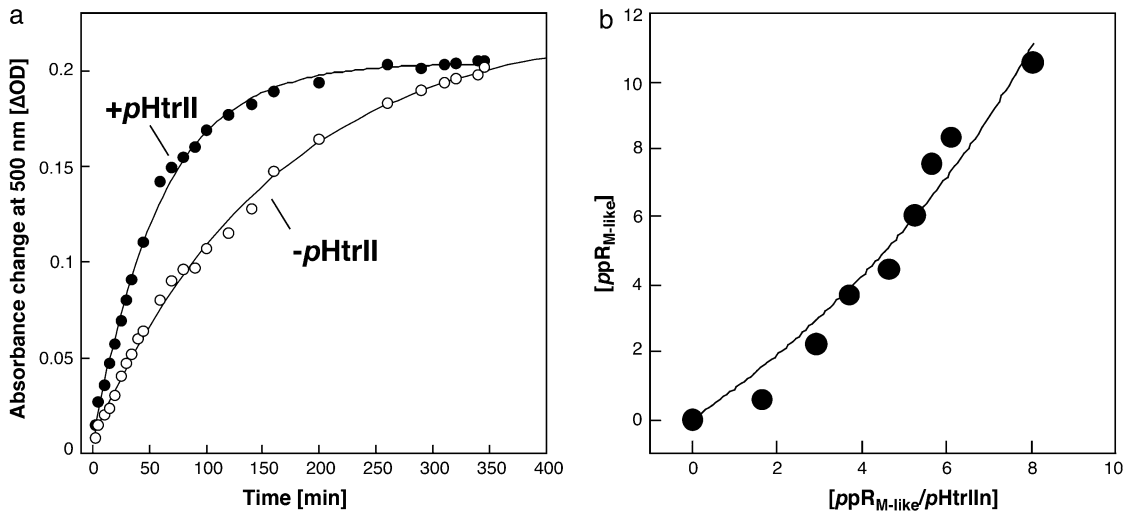

FIGURE 5 (*a*) Spectral transition from the M-like state to the ground state in the presence (*solid circles*) or absence of pHtrII (*open circles*). ppR samples (8 μM) with or without pHtrII (40 μM) were irradiated by yellow light through a Y52 filter for 360 min. The temperature was kept at 25°C. The reverse reaction from the M-like state to the ground state in the presence or absence of purified pHtrII was monitored using a UV-Vis spectrometer as an increase in absorbance at 500 nm. (*b*) Interaction between $ppR_{M\text{-}like}$ and ppR. The concentration of free $ppR_{M\text{-}lilke}$, $[ppR_{M\text{-}like}]$, and the $ppR_{M\text{-}like}$/pHtrII complex, $[ppR_{M\text{-}like}/pHtrII]$, were calculated according to Eqs. 1–3 and are expressed as micromolar. The solid line represents the fit curve. Data were regressed with nonlinear regression Origin software to evaluate K_D and n, which were 5.2 μM and 0.7, respectively.

$$ppR_{M\text{-}like}/pHtrII_n \leftrightarrow ppR_{M\text{-}like} + n pHtrII \quad (2)$$

$$ppR_{dark\text{-}state}/pHtrII_n \leftrightarrow ppR_{dark\text{-}state} + n pHtrII, \quad (2')$$

where n represents the number of pHtrII molecules required for the formation of the complex with ppR. Here there are two assumptions: 1), The ppR and pHtrII exist as complex in Eq. 2′ because ppR tightly binds with pHtrII in the dark state with a 1:1 stoichiometry (K_D is estimated as ~100–200 nM) (16,19,29). In this case, the equilibration goes to the left side. 2), The transducer-bound and free M-like states equilibrate more slowly than the lifetime of the M-like state.

The dissociation constant should be defined as:

$$K_D = \{[ppR_{M\text{-}like}][pHtrII]^n\}/[ppR_{M\text{-}like}/pHtrII_n]. \quad (3)$$

The mass balance equations for pHtrII and ppR are

$$n[ppR_{M\text{-}like}/pHtrII] + [pHtrII] = [pHtrII]_0 \quad (4)$$

$$[ppR_{M\text{-}like}] + [ppR_{M\text{-}like}/pHtrII_n] = [ppR_{M\text{-}like}]_0, \quad (5)$$

where $[pHtrII]_0$ and $[ppR_{M\text{-}like}]_0$ stand for the total concentration of pHtrII and ppR, respectively.

$[pHtrII]_0$ and $[ppR_{M\text{-}like}]_0$ were estimated by mass balance as follows:

$$[pHtrII]_0 = [pHtrII_{total}] - [ppR_{dark\text{-}state}/pHtrII]$$

$$[ppR_{M\text{-}like}]_0 = [ppR_{total}] - [ppR_{dark\text{-}state}/pHtrII],$$

where $[pHtrII_{total}]$ and $[ppR_{total}]$ were given by initial concentrations (i.e., $[pHtrII_{total}] = 25$ μM, $[ppR_{total}] = 5$, 10, 15, 20, 25, 30, 35, or 40 μM), and $[ppR_{dark\text{-}state}/pHtrII]$ was given by absorbance at 500 nm before the measurements.

As described above, the amplitudes of Eq. 1 are assumed to be

$$c/d = [ppR_{M\text{-}like}]/[ppR_{M\text{-}like}/pHtrII_n]. \quad (6)$$

The combination of Eqs. 5 and 6 yielded $[ppR_{M\text{-}like}]$ and $[ppR_{M\text{-}like}/pHtrIIn]$ for every point of the titration data. The solid circles in Fig. 5 *b* represent the free $ppR_{M\text{-}like}$ concentration $[ppR_{M\text{-}like}]$ plotted against the complex concentration $[ppR_{M\text{-}like}/pHtrIIn]$ calculated with Eq. 4 and k_1 and k_2. The increase in $[ppR_{M\text{-}like}]$ was initially small on the addition of $ppR_{M\text{-}like}$, which means that the added $ppR_{M\text{-}like}$ associated with pHtrII to form the complex when $ppR_{M\text{-}like}$ was dilute. Above ~5 μM $[ppR_{M\text{-}like}/pHtrIIn]$, the concentration of free $ppR_{M\text{-}like}$ increased abruptly, suggesting a K_D value of ~5 μM. The elimination of [pHtrII] from Eq. 3 and 4 gave an equation that expresses the relation of $[ppR_{M\text{-}like}]$ against $[ppR_{M\text{-}like}/pHtrIIn]$, as shown in Fig. 5 *b*. Nonlinear regression gave a K_D-value of 5.2 ± 1.1 and an n-value of 0.7 ± 0.1.

pK_a of the Schiff base at the M-like state

After the constant illumination, the pH was adjusted to 1.2 using concentrated H_2SO_4 and a mixture of six buffers (see Materials and Methods). On addition of H_2SO_4, the λ_{max} of ppR shifted to ~470 nm because the retinal Schiff base was protonated in the M-like state. The intermediate having the PSB was named the ''P-state''. The pH titration of the PSB started from 1.2 to 3.9 and was adjusted by the addition of concentrated NaOH, and the absorption spectra were then measured. The absorbance of the P-state does not change for at least 1 h, implying the high stability of the P-state during the pH titration. Fig. 6 *a* shows absorption spectra of the M-like state at varying pH. Fig. 6, *b* and *c*, show the absor-

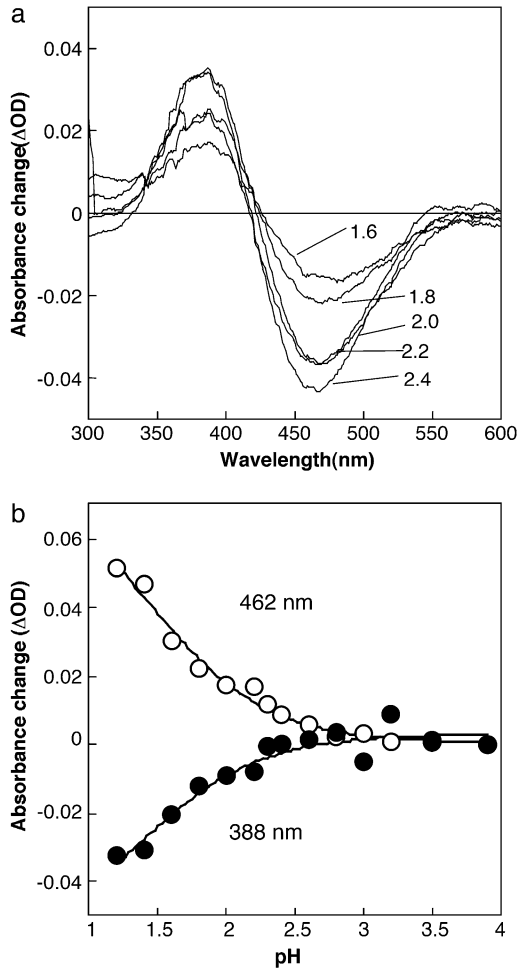

FIGURE 6 Estimation of pK_a value of the Schiff base. (*a*) pH titration of the Schiff base in $ppR_{M\text{-}like}$. Changes in absorption spectra of protonated M-like state from 1.2 to 3.9 were monitored. The pH values of each spectrum are 2.4, 2.2, 2.0, 1.8, and 1.6, respectively. (*a* and *b*) Estimated absorbance changes using spectral deconvolution at 388 and 462 nm, respectively. Experimental conditions were as reported for Fig. 1 except for the salt concentration (0 mM). The plots are based on three or four independent experiments.

bance changes at 388 and 462 nm, respectively, which implies that the absorption maximum of the pigment having the PSB was 462 nm. Deconvolution of the difference spectra revealed that the exact absorption maximum are 388 and 462 nm for the M-like and the P-state, respectively (data not shown). We plotted absorbance changes at 462 and 388 nm against pH. The decrease of absorbance change at 462 and the increase of absorbance change at 388 nm indicate a spectral transition from the P-state having the PSB to the M-like state having the PSB. These pH-dependent changes were reversible and were observed even if we used the sample after the measurement. Therefore, these pH dependencies do not originate from the protein denaturation. The data fit well with the Henderson-Hasselbalch equation with a single pK_a of 1.5 ± 0.2. The pK_a value at the ground state of ppR is reported as <12 (30). By this decrease of pK_a, proton movement occurs from the PSB to the counterion, Asp-75. That proton movement may be the trigger not only for the proton pumping but also for the signal transduction. For the fitting, the Hill coefficients were held to 1. Although the data fit well, it should be noted that besides the Schiff base there are other residues that might be titratable at this pH range and that might affect the absorption maximum.

DISCUSSION

Detecting the M-like state

In this study, we identified a new photointermediate that is highly stable (half-time is ~2 h). Why is the M-like state so highly stable? In this study, we used OG as a detergent. The M-like state was not trapped in other detergents, i.e., *n*-dodecyl-β-D-maltoside or cholic acid (data not shown). As shown for other retinal proteins, OG perturbs their properties, such as the pK_as of the Schiff base and the counterion, to a substantially larger extent than does *n*-dodecyl-β-D-maltoside as an example. This may be at least one reason for the formation of the long-lived M-like state in ppR.

HPLC analysis reveals that this stable state has 13-*cis*-retinal as its chromophore, and characterization of its reaction with hydroxylamine reveals that the overall protein structure of the M-like state is similar to that of the M-state during the ppR photocycle. For photoactive proteins, many interesting results have been reported utilizing highly stable properties (31,32). For instance, a M100L mutant of PYP (a small water-soluble photoreceptor protein found in several eubacterial strains) was stabilized to the PYPM-like state, which allowed various experiments that require a long measurement time (33,34). In fact, various studies were performed, and the activation mechanism of PYP has been well characterized over the past few years.

Transducer binding and pK_a of the Schiff base

The M and the M-like decay rates of ppR are ~1.6 s^{-1} and 2 h^{-1} (half-time), respectively. Thus, the M-like state is ~5000-fold more stable than the M-state during the photocycle. We analyzed the interaction between $ppR_{M\text{-}like}$ and pHtrII and estimated the pK_a value of the Schiff base at the M-like state.

In the dark state, ppR binds to pHtrII with a dissociation constant of ~0.1–0.2 μM (16,19). In this study, the K_D of $ppR_{M\text{-}like}$/pHtrII was estimated to be 5 μM, suggesting that the interaction between ppR_M and pHtrII became ~25–50-fold weaker than that of the ground state ppR and pHtrII. Why is the interaction between $ppR_{M\text{-}like}$ and pHtrII so weak? Recently, we and other groups reported the importance of the pHtrII linker region ($pHtrII^{G83\text{–}Q149}$) for the interaction with ppR (19,35,36). Thus, we propose that the interaction might be broken at the M-state. FTIR spectra of

the transmembrane helices of pHtrII do not change so much in the complex with ppR_M from the ground state of the ppR/pHtrII complex (37). Therefore, the pHtrII linker region is perturbed by the M-state of ppR, that is, the interaction between ppR and pHtrII becomes weak. Wegener et al. (38) reported that the helix-F of ppR moves toward pHtrII by the light activation of ppR. The movement of the helix during the photocycle in bR has also been reported (39). This helix movement of ppR is the signaling trigger to pHtrII. Actually, Engelhard and co-workers (40) have reported that the TM-2 of pHtrII rotates by the helix movement of ppR. These structural changes induce the changes in interaction between ppR and pHtrII. For instance, the hydrogen bond between $Tyr\text{-}199^{ppR}$ and $Asn\text{-}74^{pHtrII}$, which is quite important for the association between ppR and pHtrII, is disrupted on formation of the M-intermediate as reported by Bergo et al. (41), although there are no significant changes in the crystal structure of M-intermediate of ppR. By using mutants and/or chimeras, the important residue(s) for weaker binding should be investigated.

In this study, we estimated the pK_a of the Schiff base of ppR_M. Both bR and ppR act as proton pumps (42,43). On formation of bR_M and ppR_M during the photocycle, the primary proton transfer from the PSB ($pK_a = 1.5 \pm 0.2$) to its counterion, Asp-85 for bR and Asp-75 for ppR (pK_a value is $\sim$5 at the ground state of ppR), and subsequent proton release from the proton-releasing group to the extracellular side, occur. It is believed that this primary proton transfer plays a crucial role in the proton pumping of bR and ppR. In fact, counterion mutants (D85N of bR and D75N of ppR) cannot transfer protons from the cytoplasmic side to the extracellular side. We first determined the pK_a value of the Schiff base at the M state, although computational experiments had been done. The decrease of pK_a of the Schiff base from 12 to 1.5 is essentially important for the proton transfer mechanism. We reported that the proton-pumping activity ceases on association with pHtrII. The pK_a value of the Schiff base may change by the complex formation. Further, how does the protonation of the Schiff base affect the kinetics of recovery and interaction with the transducer? Does neutralization of the counterion by the D75N mutation affect the behavior of the long-lived photoproduct? These are quite interesting questions that remain to be examined.

In conclusion, we discovered that the M-like state has 13-*cis*-retinal and a protein conformation similar to the M state during the photocycle. From binding assays between $ppR_{M\text{-}like}$ and pHtrII, the interaction between ppR_M and pHtrII became $\sim$25–50-fold weaker than that of the ground state ppR and pHtrII. The association/dissociation or conformational changes of the pHtrII linker region occur at the M state, which may be one reason for the weak interaction. From the pH titration measurement, we first estimated the pK_a value of the Schiff base in the intermediate. This decrease of pK_a is essential for the proton transfer mechanism in retinal proteins.

This work was supported by grants from the Japanese Ministry of Education, Culture, Sports, Science, and Technology.

REFERENCES

1. Spudich, J. L., C.-S. Yang, K.-H. Jung, and E. N. Spudich. 2000. Retinylidene proteins: structures and functions from archaea to humans. *Annu. Rev. Cell Biol.* 16:365–392.
2. Sudo, Y., H. Kandori, and N. Kamo. 2004. Molecular mechanism of protein-protein interaction of *pharaonis* phoborhodopsin/transducer and photo-signal transfer reaction by the complex. *Recent Res. Devel. Biophys.* 3:1–16.
3. Falke, J. J., R. B. Bass, S. L. Butler, S. A. Chervitz, and M. A. Danielson. 1997. The two-component signaling pathway of bacterial chemotaxis: a molecular view of signal transduction by receptors, kinases, and adaptation enzymes. *Annu. Rev. Cell Dev. Biol.* 13:457–512.
4. Rudolph, J., and D. Oesterhelt. 1996. Deletion analysis of the che operon in the archaeon *Halobacterium salinarium*. *J. Mol. Biol.* 258: 548–554.
5. Ikeura, Y., K. Shimono, M. Iwamoto, Y. Sudo, and N. Kamo. 2003. Arg-72 of *pharaonis* phoborhodopsin (sensory rhodopsin II) is important for the maintenance of the protein structure in the solubilized state. *Photochem. Photobiol.* 77:96–100.
6. Sudo, Y., M. Yamabi, M. Iwamoto, K. Shimono, and N. Kamo. 2003. Interaction of *Natronobacterium pharaonis* phoborhodopsin (sensory rhodopsin II) with its cognate transducer probed by increase in the thermal stability. *Photochem. Photobiol.* 78:511–516.
7. Shimono, K., M. Iwamoto, M. Sumi, and N. Kamo. 1997. Functional expression of *pharaonis* phoborhodopsin in *Escherichia coli*. *FEBS Lett.* 420:54–56.
8. Klare, J. P., E. Bordignon, M. Engelhard, and H. J. Steinhoff. 2004. Sensory rhodopsin II and bacteriorhodopsin: light activated helix F movement. *Photochem. Photobiol. Sci.* 3:543–547.
9. Royant, A., P. Nollert, K. Edman, R. Neutze, E. M. Landau, E. Pebay-Peyroula, and J. Navarro. 2001. X-ray structure of sensory rhodopsin II at 2.1-A resolution. *Proc. Natl. Acad. Sci. USA.* 98:10131–10136.
10. Luecke, H., B. Schobert, J. K. Lanyi, E. N. Spudich, and J. L. Spudich. 2001. Crystal structure of sensory rhodopsin II at 2.4 angstroms: insights into color tuning and transducer interaction. *Science.* 293: 1499–1503.
11. Gordeliy, V. I., J. Labahn, R. Moukhametzianov, R. Efremov, J. Granzin, R. Schlesinger, G. Bult, T. Savopol, A. Scheidig, J. P. Klare, and M. Engelhard. 2002. Molecular basis of transmembrane signalling by sensory rhodopsin II- transducer complex. *Nature.* 419:484–487.
12. Moukhametzianov, R., J. P. Klare, R. Efremov, C. Baeken, A. Göppner, J. Labahn, M. Engelhard, G. Büldt, and V. I. Gordeliy. 2006. Development of the signal in sensory rhodopsin and its transfer to the cognate transducer. *Nature.* 440:115–119.
13. Sudo, Y., M. Iwamoto, K. Shimono, and N. Kamo. 2001. *Pharaonis phoborhodopsin* binds to its cognate truncated transducer even in the presence of a detergent with a 1:1 stoichiometry. *Photochem. Photobiol.* 74:489–494.
14. Chen, X., and J. L. Spudich. 2002. Demonstration of 2:2 stoichiometry in the functional SRI-HtrI signaling complex in Halobacterium membranes by gene fusion analysis. *Biochemistry.* 41:3891–3896.
15. Sudo, Y., M. Iwamoto, K. Shimono, and N. Kamo. 2002. Tyr-199 and charged residues of *pharaonis* phoborhodopsin are important for the interaction with its transducer. *Biophys. J.* 83:427–432.
16. Hippler-Mreyen, S., J. P. Klare, A. A. Wegener, R. Seidel, C. Herrmann, G. Schmies, G. Nagel, E. Bamberg, and M. Engelhard. 2003. Probing the sensory rhodopsin II binding domain of its cognate transducer by calorimetry and electrophysiology. *J. Mol. Biol.* 330: 1203–1213.
17. Sudo, Y., Y. Furutani, K. Shimono, N. Kamo, and H. Kandori. 2003. Hydrogen bonding alteration of Thr-204 in the complex between

pharaonis phoborhodopsin and its transducer protein. *Biochemistry.* 42:14166–14172.

18. Sudo, Y., M. Iwamoto, K. Shimono, and N. Kamo. 2004. Role of charged residues of *pharaonis* phoborhodopsin (sensory rhodopsin II) in its interaction with the transducer protein. *Biochemistry.* 43:13748–13754.
19. Sudo, Y., H. Okuda, M. Yamabi, Y. Fukuzaki, M. Mishima, N. Kamo, and C. Kojima. 2005. Linker region of a Halobacterial transducer protein interacts directly with its sensor retinal protein. *Biochemistry.* 44:6144–6152.
20. Shimono, K., T. Hayashi, Y. Ikeura, Y. Sudo, M. Iwamoto, and N. Kamo. 2003. Importance of the broad regional interaction for spectral tuning in *Natronobacterium pharaonis* phoborhodopsin (sensory rhodopsin II). *J. Biol. Chem.* 278:23882–23889.
21. Yan, B., T. Takahashi, R. Johnson, and J. L. Spudich. 1991. Identification of signaling states of a sensory receptor by modulation of lifetimes of stimulus-induced conformations: the case of sensory rhodopsin II. *Biochemistry.* 30:10686–10692.
22. Iwamoto, M., Y. Sudo, K. Shimono, and N. Kamo. 2001. Selective reaction of hydroxylamine with chromophore during the photocycle of *pharaonis* phoborhodopsin. *Biochim. Biophys. Acta.* 1514:152–158.
23. Sudo, Y., M. Iwamoto, K. Shimono, and N. Kamo. 2002. Association of *pharaonis* phoborhodopsin with its cognate transducer decreases the photo-dependent reactivity by water-soluble reagents of azide and hydroxylamine. *Biochim. Biophys. Acta.* 1558:63–69.
24. Sudo, Y., M. Iwamoto, K. Shimono, and N. Kamo. 2002. Association between a photo-intermediate of a M-lacking mutant D75N of *pharaonis* phoborhodopsin and its cognate transducer. *J. Photochem. Photobiol. B.* 67:171–176.
25. Shimono, K., Y. Ikeura, Y. Sudo, M. Iwamoto, and N. Kamo. 2001. Environment around the chromophore in *pharaonis* phoborhodopsin: mutation analysis of the retinal binding site. *Biochim. Biophys. Acta.* 1515:92–100.
26. Imasheva, E. S., K. Shimono, S. Pl Balashov, J. M. Wang, U. Zadok, M. Sheves, N. Kamo, and J. K. Lanyi. 2005. Formation of a long-lived photoproduct with a deprotonated Schiff base in proteorhodopsin, and its enhancement by mutation of Asp227. *Biochemistry.* 44:10828–10838.
27. Chizhov, I., G. Schmies, R. Seidel, J. R. Sydor, B. Luttenberg, and M. Engelhard. 1998. The photophobic receptor from *Natronobacterium pharaonis*: temperature and pH dependencies of the photocycle of sensory rhodopsin II. *Biophys. J.* 75:999–1009.
28. Furutani, Y., M. Iwamoto, K. Shimono, N. Kamo, and H. Kandori. 2002. FTIR spectroscopy of the M photointermediate in *pharaonis* phoborhodopsin. *Biophys. J.* 83:3482–3489.
29. Sudo, Y., M. Yamabi, S. Kato, C. Hasegawa, M. Iwamoto, K. Shimono, and N. Kamo. 2006. Importance of specific hydrogen bonds of archaeal rhodopsins for the binding to the transducer protein. *J. Mol. Biol.* 357:1274–1282.
30. Iwamoto, M., Y. Furutani, Y. Sudo, K. Shimono, H. Kandori, and N. Kamo. 2002. Role of Asp193 in chromophore-protein interaction of *pharaonis* phoborhodopsin (Sensory rhodoopsin II). *Biophys. J.* 83: 1130–1135.
31. Devanathan, S., U. K. Genick, I. L. Canestrelli, T. E. Meyer, M. A. Cusanovich, E. D. Getzoff, and G. Tollin. 1998. New insights into the photocycle of *Ectothiorhodospira halophila* photoactive yellow protein: photorecovery of the long-lived photobleached intermediate in the Met100Ala mutant. *Biochemistry.* 37:11563–11568.
32. Reference deleted in proof.
33. Sasaki, J., M. Kumauchi, N. Hamada, T. Oka, and F. Tokunaga. 2002. Light-induced unfolding of photoactive yellow protein mutant M100L. *Biochemistry.* 41:1915–1922.
34. Kyndt, J. A., J. K. Hurley, B. Devreese, T. E. Meyer, M. A. Cusanovich, G. Tollin, and J. J. Van Beeumen. 2004. *Rhodobacter capsulatus* photoactive yellow protein: genetic context, spectral and kinetics characterization, and mutagenesis. *Biochemistry.* 43:1809–1820.
35. Yang, C. S., O. Sineshchekov, E. N. Spudich, and J. L. Spudich. 2004. The cytoplasmic membrane-proximal domain of the HtrII transducer interacts with the E-F loop of photoactivated *Natronomonas pharaonis* sensory rhodopsin II. *J. Biol. Chem.* 279:42970–42976.
36. Bordignon, E., J. P. Klare, M. Doebber, A. A. Wegener, S. Martell, M. Engelhard, and H. J. Steinhoff. 2005. Structural analysis of a hamp domain: The linker region of the phototransducer in complex with sensory rhodopsin II. *J. Biol. Chem.* 280:38767–38775.
37. Furutani, Y., K. Kamada, Y. Sudo, K. Shimono, N. Kamo, and H. Kandori. 2005. Structural changes of the complex between *pharaonis* phoborhodopsin and its cognate transducer upon formation of the M photointermediate. *Biochemistry.* 44:2909–2915.
38. Wegener, A. A., I. Chizhov, M. Engelhard, and H. J. Steinhoff. 2000. Time-resolved detection of transient movement of helix F in spin-labelled *pharaonis* sensory rhodopsin II. *J. Mol. Biol.* 301:881–891.
39. Radzwill, N., K. Gerwert, and H. J. Steinhoff. 2001. Time-resolved detection of transient movement of helices F and G in doubly spin-labeled bacteriorhodopsin. *Biophys. J.* 80:2856–2866.
40. Wegener, A. A., J. P. Klare, M. Engelhard, and H. J. Steinhoff. 2001. Structural insights into the early steps of receptor-transducer signal transfer in archaeal phototaxis. *EMBO J.* 20:5312–5319.
41. Bergo, V. B., E. N. Spudich, K. J. Rothschild, and J. L. Spudich. 2005. Photoactivation perturbs the membrane-embedded contacts between sensory rhodopsin II and its transducer. *J. Biol. Chem.* 280:28365–28369.
42. Lanyi, J. K., and H. Luecke. 2001. Bacteriorhodopsin. *Curr. Opin. Struct. Biol.* 11:415–419.
43. Sudo, Y., M. Iwamoto, K. Shimono, M. Sumi, and N. Kamo. 2001. Photo-induced proton transport of *pharaonis* phoborhodopsin (sensory rhodopsin II) is ceased by association with the transducer. *Biophys. J.* 80:916–922.